J. Mol. Biol. (1995) **251**, 563–573

JMB

The Three-dimensional Crystal Structure of Cholera Toxin

Rong-Guang Zhang[1], David L. Scott[2], Mary L. Westbrook[1] Sharon Nance[1], Brenda D. Spangler[1], G. Graham Shipley[3] and Edwin M. Westbrook[1,4]*

[1]*Center for Mechanistic Biology and Biotechnology Argonne National Laboratory Argonne, IL, 60439, USA*

[2]*Department of Molecular Biophysics and Biochemistry Yale University, New Haven CT 06511, USA*

[3]*Department of Biophysics Boston University School of Medicine, Boston, MA 02118 USA*

[4]*Department of Biochemistry Molecular Biology, and Cell Biology, Northwestern University, Evanston IL 60602, USA*

**Corresponding author*

The clinical manifestations of cholera are largely attributable to the actions of a secreted hexameric AB_5 enterotoxin (choleragen). We have independently solved and refined the three-dimensional structure of choleragen at 2.5 Å resolution. The structure of the crystalline toxin closely resembles that described for the heat-labile enterotoxin from *Escherichia coli* (LT) with which it shares 80% sequence homology. In both cases, the wedge-shaped A subunit is loosely held high above the plane of the pentameric B subunits by the tethering A2 chain. The most striking difference between the two toxins occurs at the carboxyl terminus of the A2 chain. Whereas the last 14 residues of the A2 chain of LT threading through the central pore of the B_5 assembly form an extended chain with a terminal loop, the A2 chain of choleragen remains a nearly continuous α-helix throughout its length. The four carboxyl-terminal residues of the A2 chain (KDEL sequence), disordered in the crystal structure of LT, are clearly visible in choleragen's electron-density map.

In the accompanying article we describe the three-dimensional structure of the isolated B pentamer of cholera toxin (choleragenoid). Comparison of the crystalline coordinates of choleragen, choleragenoid, and LT provides a solid three-dimensional foundation for further experimental investigation. These structures, along with those of related toxins from *Shigella dysenteria* and *Bordetella pertussis*, offer a first step towards the rational design of new vaccines and anti-microbial agents.

© 1995 Academic Press Limited

Keywords: crystal structure; cholera toxin; choleragenoid; enterotoxins; ADP-ribosylation

Introduction

The massive fluid release accompanying infection with large numbers of *Vibrio cholerae* results from the secretion of a potent bacterial enterotoxin (Finkelstein, 1988; Moss & Vaughan, 1988; Cassel & Pfeuffer, 1978; De, 1959). Cholera toxin is a heterohexameric AB_5 complex (M_r = 85,620) that binds cooperatively *via* its pentameric B subunits to GM_1 gangliosides exposed on the luminal surface of intestinal epithelial cells (Sattler *et al*., 1978). Activation of the enzymatic A subunit requires proteolytic cleavage between residues 192 and 194 followed by reduction of a single disulfide bond (Cys187 = Cys199). The liberated A1 fragment (residues 1 to 192 or 1 to 194), passes through the membrane where it interacts with one or more cytosolic factors (Moss *et al*., 1994; Moss & Vaughan, 1991; Janicot *et al*., 1991; Kassis *et al*., 1982; Mekalanos *et al*., 1979). The internalized A1 complex binds NAD and catalyzes the ADP-ribosylation of $G_{s\alpha}$, a GTP-binding regulatory protein associated with adenylate cyclase (Galloway & van Henyningen, 1987). Activation of intestinal sodium pumps *via* a cyclic AMP-dependent protein kinase precipitates the massive influx of sodium and water into the gut lumen (Peterson & Ochoa, 1989). The resulting diarrhea often exceeds six liters per hour.

Abbreviations used: CT, cholera toxin (choleragen); CTB, B subunit pentamer of cholera toxin (choleragenoid); LT, heat-labile enterotoxin from *Escherichia coli*; ST, shiga toxin; PT, pertussis toxin; VT, verotoxin; GM_1, Galβ1-3GalNAcβ1-(NeuAcα2-3)4Galβ1-4Glcβ1-ceramide; r.m.s., root-mean-square.

Present address: D. L. Scott, Medical Services, Massachusetts General Hospital, Boston, MA 02114, USA.

Present address: B. D. Spangler, Department of Biological Sciences and Department of Chemistry, Northern Illinois University, Dekalb, IL 60115, USA.

0022–2836/95/340563–11 $12.00/0

© 1995 Academic Press Limited

Cholera toxin (CT) belongs to a class of microbial toxins that are composed of structurally independent A (enzymatic) and B (targeting) subunits (reviewed by Spangler, 1992; Burnette, 1994). The refined crystal structures of several other A-B toxins including *Pseudomonas aeruginosa* exotoxin A, *Escherichia coli* heat-labile enterotoxin (LT), the B pentamer of *Escherichia coli* verotoxin-1, shiga toxin, pertusis toxin, and diphtheria toxin have been reported (Allured *et al*., 1986; Carroll & Collier, 1987; Sixma *et al*., 1991, 1993; Stein *et al*., 1992, 1994; Fraser *et al*., 1994; Choe *et al*., 1992). Co-crystals of LT with lactose and CT with GM_1 ganglioside have proven particularly helpful in clarifying the mechanism by which AB_5 toxins interact with their cell surface receptors (Sixma *et al*., 1992a,b; Merritt *et al*., 1994a).

The genomes of enterotoxic strains of *V. cholera* and *E. coli* encode for structurally and functionally similar toxins. As illustrated in Figure 1, the A and B cistrons of the chromosomal CT gene are 75% and 77% homologous, respectively, with those of the plasmid-borne LT enterotoxin (Dykes *et al*., 1985; Tsuji *et al*., 1984; Lockman & Kaper, 1983; Mekalanos *et al*., 1983; Dallas, 1983; Dallas & Falkow, 1980; Kurosky *et al*., 1977). Differences in the inferred amino acid sequences for the A subnits are greatest near the A1 / A2 cleavage site where the homology drops to 33% between amino acid residues 189 and 212.

As anticipated from the high sequence homology, the three-dimensional structures of CT and LT are quite similar. In both cases the wedge-shaped A1 subunit is loosely held high above the plane of the pentameric ring of B subunits by the tethering A2 chain (Figure 2). Comparison of the coordinates of the proteolytically ''nicked'' CT with those of either the nicked (Merritt *et al*., 1994b) or intact LT (Sixma *et al*., 1993) reveals little structural effect of nicking on the holotoxin. The most striking difference between CT and LT occurs at the carboxyl terminus of the A2 chain. Whereas the last 14 residues of the A2 chain of LT form an extended chain with a terminal loop, the A2 chain of choleragen remains a nearly continuous α-helix throughout its length.

Results and Discussion

Overall structure

The refined model of cholera holotoxin (choleragen) includes all protein atoms with the exception of three residues at the A1–A2 cleavage site (residues A: 193 to 195). The overall quality of the electron-density map is crisp (Figure 3); however, the densities for residues A:192 and A:237 to 240 are incomplete. Over 100 well-refined solvent molecules are included at the current limited resolution suggesting that cholera

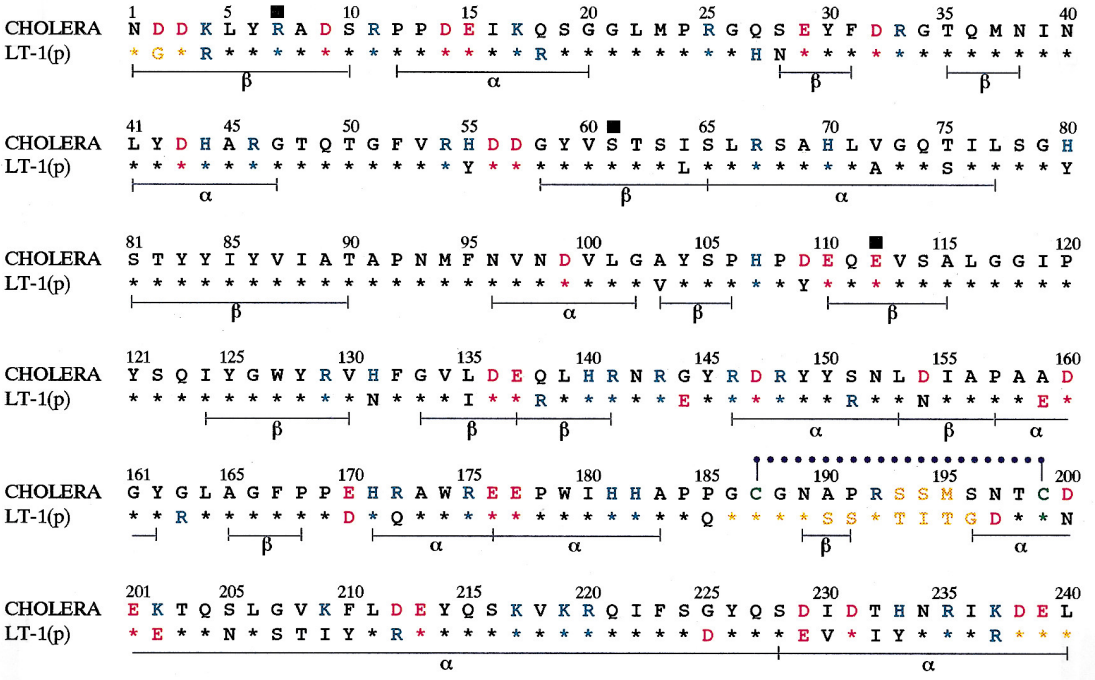

Figure 1. Comparison of the amino acid sequences of the A subunits of cholera (CT) and heat-labile (LT) enterotoxins (Dykes *et al.*, 1985; Kurosky *et al.*, 1977; Tsuji *et al.*, 1984; Mekalanos *et al.*, 1983; Lockman & Kaper, 1983; Dallas & Falkow, 1980). The LT isozyme shown here corresponds to that present in the crystal structure (Sixma *et al.*, 1991, 1993). Asterisks occupy positions of sequence identity: secondary structure for CT is noted below the corresponding sequence segment (Richards & Kundrot, 1988). Acidic residues (Asp and Glu) are typeset in red, basic residues (Lys, Arg, and His) are shown in blue, and regions not observed in the respective crystal structures are colored yellow. Filled squares denote residues implicated in catalysis (Galloway & van Heyningen, 1987; Allured *et al.*, 1986; Carroll & Collier, 1987; Tomasi *et al.*, 1979; Lai *et al.*, 1983; Tsuji *et al.*, 1991; Burnette *et al.*, 1991; Harford *et al.*, 1989); the single disulfide bridge is shown by a dotted line.

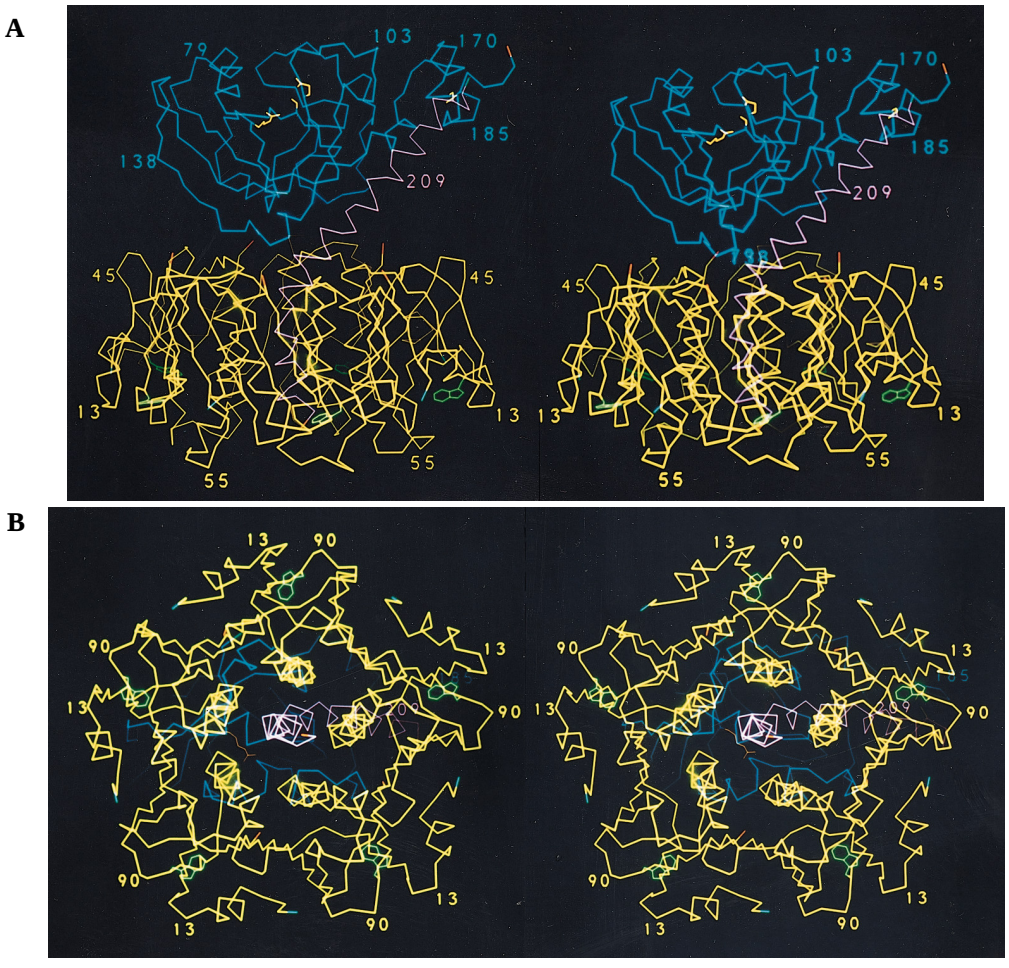

Figure 2. Overview of the crystal structure of cholera toxin. A, α-Carbon trace of the nicked AB_5 toxin emphasizing functional features. The green side-chains of B:Trp88 indicate the position of the ganglioside-binding site on each of the yellow B subunits. The A1 (blue) and A2 (magenta) chains are shown joined by their single disulfide bridge (yellow). Three residues of the A1 chain (Arg7, Ser61, and Glu112) are included in gold to indicate the crevice where NAD binding and catalysis is thought to occur (Galloway & van Heyningen, 1987; Allured *et al.*, 1986; Carroll & Collier, 1987; Tomasi *et al.*, 1979; Lai *et al.*, 1983; Tsuji *et al.*, 1991; Burnette *et al.*, 1991; Harford *et al.*, 1989). Amino and carboxyl termini are colored cyan and red, respectively. Note the limited contact surface between the A1 chain and the B pentamer and the tethering action of the A2 chain. B, Representation of CT similar to that shown in A but rotated 90° to reveal the ventral surface. The five long α-helices (residues B:58 to 79) surrounding the central pore of the B pentamer form a tight cage around the interposed A2 α-helix. Residues 236 to 240 of the A2 chain (KDEL) emerge from the ventral surface of the B pentamer where they may contact the membrane surface.

toxin is highly hydrated under natural conditions. The three-dimensional coordinates of choleragen agree well with previous low-resolution models derived from electron microscopy (Cabral-Lilly *et al*., 1994; Mosser *et al*., 1992; Ribi *et al*., 1988; Reed *et al*., 1987), atomic force microscopy (Yang *et al*., 1993), and infrared spectroscopy (Surewicz *et al*., 1990).

The B (binding) subunit

As discussed in the accompanying article (Zhang *et al*., 1995), the B subunits of CT form a highly stable pentamer (choleragenoid) with nearly perfect 5-fold symmetry. The central cylindrical pore (11 Å diameter × 40 Å long) is lined by five amphipathic α-helices that are intimately involved in pentamer stabilization (Figure 2). The pentamer contains five equivalent GM_1 binding sites with measured dissociation constants ranging from 10^{-9} to 10^{-10} M depending upon the analytical technique (Fishman *et al*., 1978; Ludwig *et al*., 1986; Reed *et al*., 1987). Small angle X-ray diffraction studies suggest that in the absence of ligand the negatively charged pentasaccharide of GM_1 (Gal-β-1-3-GalNAc-β1-(NeuAc-α2-3)-4Gal-β1-4-Glc-β1-ceramide) lies nearly 21 Å above the lipid/water interface (McDaniel & McIntosh, 1986). Co-crystals of LT with lactose (Gal-β1-4-Glc), and of choleragenoid with galactose or with GM_1 oligosaccharide have shown that the distal saccharides of GM_1 bind to a small cleft adjacent to B:Trp88 on the ventral flange of the B pentamer (Sixma *et al*., 1992; Zhang *et al*., 1995; Merritt *et al*., 1994a). Based on simple geometric constraints it is likely that choleragen binds to GM_1 with its B pentamer facing towards the membrane surface. Electron micrographs of two-dimensional

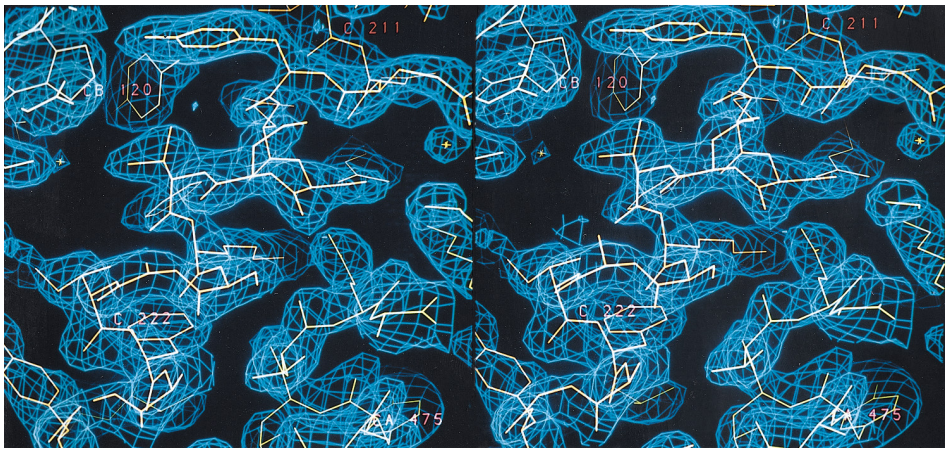

Figure 3. Representative electron-density for cholera toxin. Stereo view of the $2F_o–F_c$ electron-density map at the junction between the A subunit and the B pentamer. The long A2 α-helix (orange) can be seen as it begins its descent into the central pore. Residues belonging to the A1 chain or to the B pentamer are indicated (Pro120 and Ala(4)75, respectively).

crystals of cholera toxin bound to GM_1-containing bilayers show a convincing volume of electron-density lying above the B pentamer opposite to the binding surface (Cabral-Lilly *et al*., 1994). Several plausible mechanisms have been proposed to explain cholera toxin's subsequent internalization (Spangler, 1992).

The A (catalytic) subunit—overview

The A subunit of CT is loosely folded with almost complete loss of secondary structure occurring above 46°C (Surewicz *et al*., 1990). The A subunit is translated as a single 240 amino acid protein that is nicked by a bacterial endoprotease to form two chains (A1 and A2) prior to internalization (Tomasi *et al*., 1979). Given the large distance (9 Å) and the improbable geometry between the observed A1 carboxyl terminus (Arg192) and the amino terminus of the A2 fragment (Ser196), it is likely that the crystallized protein has already undergone proteolytic processing (Figure 4). The two chains of the nicked A subunit remain held together by extensive non-covalent forces and the single intrachain disulfide bond (Cys187 = Cys199).

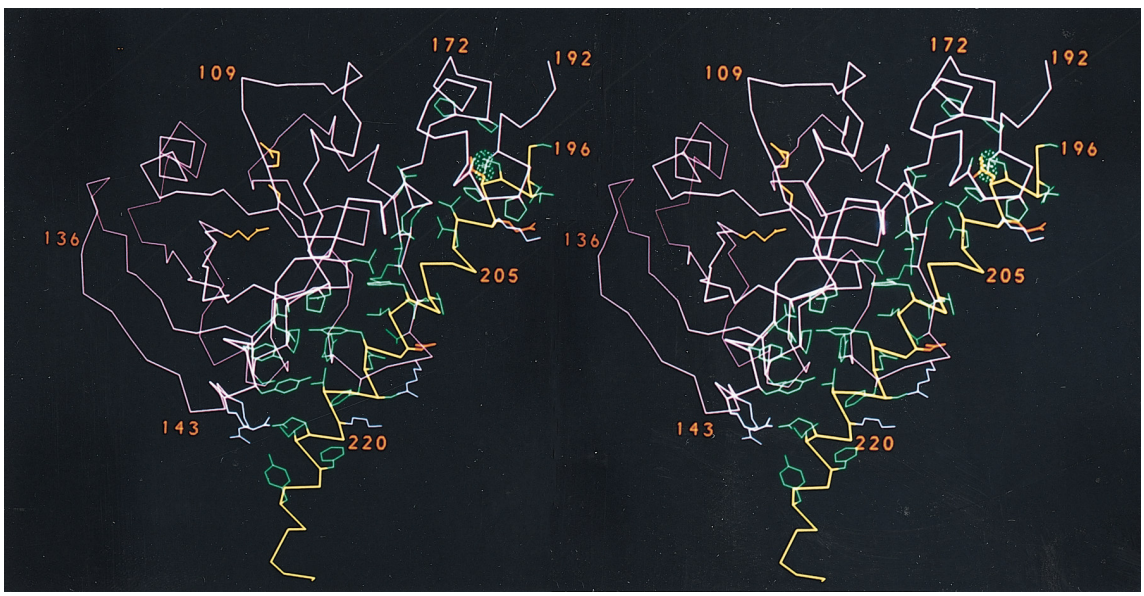

Figure 4. Detail of the A1–A2 interface of cholera toxin. The A1 chain (residues 1 to 194) and the A2 chain (residues 195 to 240) are synthesized as a single polypeptide that is subsequently cleaved by either a microbial (CT) or host (LT) associated protease. After cleavage, the two fragments remain associated almost entirely by non-polar interactions as well as by a single disulfide bridge (Cys187 = Cys199). The orientation shown here is similar to that of Figure 2. The A1 chain is shown in lavendar and the A2 chain in yellow. Side-chains contributing to the A1–A2 interface are colored according to charge: green, non-polar; red, negatively charged; blue, positively charged. Residues directly implicated in catalysis (Arg7 and Glu61) are also indicated (gold).

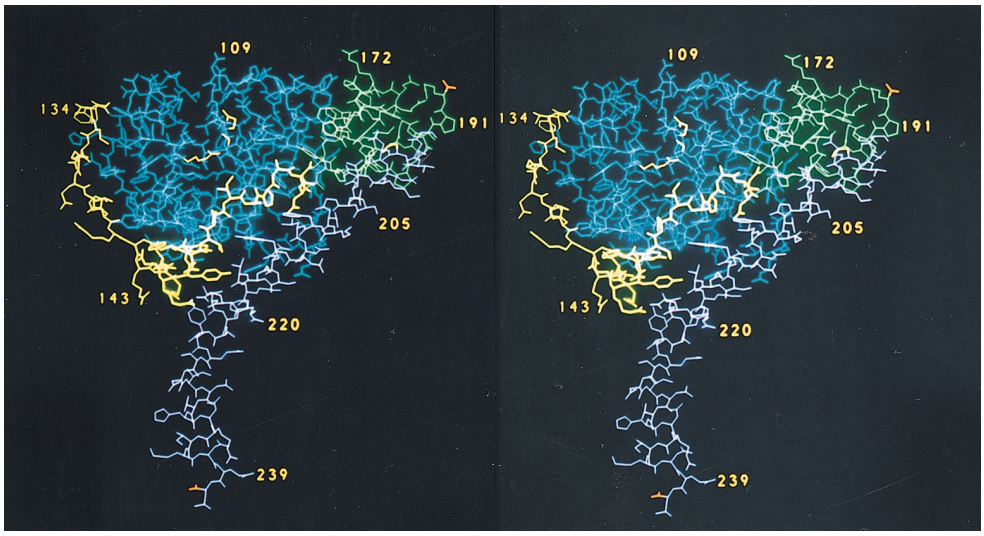

Figure 5. View of the A subunit demonstrating the two A chains and their contact surface. The orientation chosen is similar to that shown in Figure 2A. The A1 chain can be divided into three substructures: a globular amino terminus that includes the catalytic residues ($A1_1$, blue), a linking bridge of residues ($A1_2$, gold), and a second globular region ($A1_3$, green). The A2 chain (magenta) is composed of two contiguous helices that form an angle of 52°. The amino-terminal helix of A2 lies in a shallow groove along the ventral surface of the A1 chain and is anchored proximally by a disulfide bridge (yellow). The second half of the A2 helix lies almost entirely within the central pore of the B pentamer.

The A1 chain

The A1 chain is both an ADP-ribosyltransferase and a NAD-glycohydrolase catalyzing the reaction (NAD^+ + acceptor → ADP-ribose-acceptor + nicotinamide + H^+) (Gill & Coburn, 1987; Foster & Kinney, 1985; Moss *et al*., 1976). It is organized into three distinct structures (Figure 5). The first 132 amino acids form a compact globular unit composed of a mixture of α-helices and β-strands ($A1_1$). In CT, the amino-terminal nitrogen hydrogen bonds to the backbone carbonyl oxygen of residue 153 stabilizing a helix-strand transition. The absence of equivalent electron density in the crystal structure of LT indicates that this region is fairly mobile. Catalysis is thought to occur in a well-defined cleft on the free

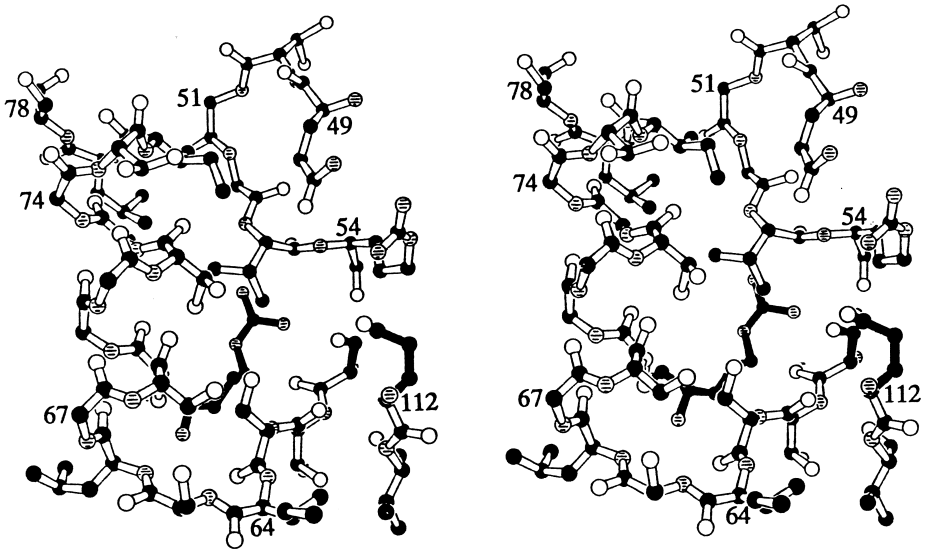

Figure 6. Schematic stereo view of the proposed catalytic site. The view presented is from the ''top'' looking down as defined for Figure 2. The residues implicated in catalyzing the NAD-dependent ADP-ribosylation of substrate line the left wall of a narrow (7 Å) cleft at the top of the A1 subunit. The cleft lacks the traditional βαβ NAD-binding fold. Both Glu112 and Ser61, which share a side-chain hydrogen bond, are important for catalysis (Galloway & van Heyningen, 1987; Allured *et al.*, 1986; Carroll & Collier, 1987; Tomasi *et al.*, 1979; Lai *et al.*, 1983; Tsuji *et al.*, 1991; Burnette *et al.*, 1991; Harford *et al.*, 1989). The side-chain of Arg7, which forms the floor of the cleft, hydrogen bonds to the backbone carbonyl oxygen of Phe52 and the side-chain carboxylate of Asp9. Replacement of Arg7 with a lysine prevents catalysis; the shorter lysine side-chain could fail to hydrogen bond with the normal partners and instead interact with Glu112. The left wall of the crevice is composed of a short stretch of charged α-helix (residues 65 to 77).

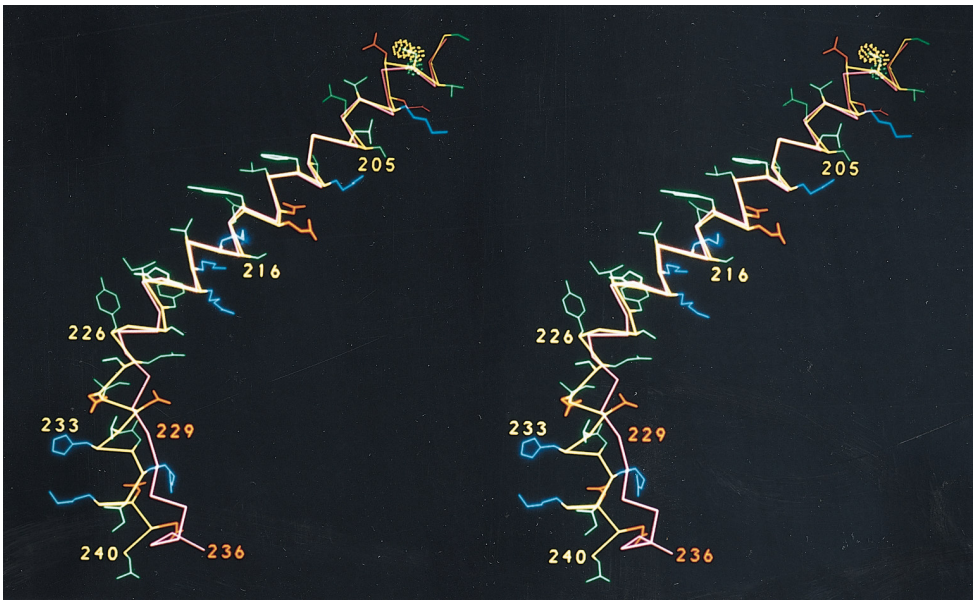

Figure 7. Least-squares superposition of the A2 chains of cholera toxin (CT) and the heat-labile enterotoxin from *E. coli* (LT). Stereo view of the α-carbon trace of LT (pink) (Sixma *et al.*, 1993) overlaid on the A2 chain of CT (gold). The side-chains of CT are colored according to charge potential (Asp, Glu = red; His, Arg, Lys = blue). Cys199 is indicated by the yellow spherical densities. The traces are essentially identical at the A1 / A2 interface but quickly diverge after each forms a 45° ''kink'' (Tyr226) in order to descend into the pore of their respective B pentamers. The A2 chain of cholera toxin remains helical throughout its course in marked contrast to the extended chain conformation of LT. Residues 237 to 240, comprising part of the HDEL / KDEL sequence, are absent from LT's electron-density map.

surface of $A1_1$ (Figure 6). This cleft is remote from both the A1 / A2 and A / B interfaces and is probably the binding site for both NAD and substrate (Tsuji *et al*., 1991; Lai *et al*., 1983; Gill, 1975).

The $A1_2$ substructure (residues 133 to 161) forms an extended bridge between the compact $A1_1$ and $A1_3$ domains. The $A1_2$ ''linker'' extends 23 Å from the distal-free face of $A1_1$ near the catalytic site to the $A1_1$ / A2 interface. Its structure suggests a role similar to that ascribed to the A2 chain, i.e. as a molecular tether. The distal $A1_2$ chain is quite flexible and becomes increasingly disordered as it approaches the nick site located along its remote free edge. Comparison of the crystalline coordinates of the nicked CT and the unnicked LT (Sixma *et al*., 1993) suggests that nicking does not in itself significantly perturb the local protein structure. The r.m.s. differences between the coordinates of CT and LT in this region are comparable to those noted between the nicked and intact forms of LT (Merritt *et al*., 1994b).

A third globular substructure ($A1_3$) is formed from the carboxy-terminal 31 residues that surround the disulfide bridge linking the A1 and A2 fragments (Figure 5). The $A1_3$ substructure is notable for its high density of hydrophobic residues including a cluster of four prolines (Pro168, Pro169, Pro184, and Pro185) and two tryptophan (Trp174 and Trp179). The $A1_1$ and $A1_2$ interface is almost entirely non-polar with only a few polar interactions occurring at the molecular surface (Figure 4). Thus, it is conceivable that at the lipid water interface the A1 subunit undergoes a substantial rearrangement that permits the $A1_1$ substructure to make contact with and / or pass through the bilayer.

The A2 chain

Cholera toxin's A2 chain, which consists of a nearly continuous α-helix broken only by a central 52 degree kink, anchors the enzymatic A1 chain to the B pentamer (Figure 7). This kink, stabilized by a hydrogen bond between the γ-oxygen of Ser228 and the peptide nitrogen of Asp229, redirects the helix prior to its descent into the pentamer pore. In contrast, the A2 chain of LT is divided into three discrete segments; a long amino-terminal helix (residues 197 to 224), a length of extended chain that winds through the pore of the B pentamer (residues 225 to 231), and a small carboxyl-terminal helix (residues 232 to 236^+) (Sixma *et al*., 1993). Intriguingly, the sequences of the last four residues of the A2 chains of both CT (KDEL) and LT (HDEL) mimic that of an endoplasmic retention signal (Lewis & Pelham, 1990; Joseph *et al*., 1978, 1979). The ''KDEL'' residues lie outside the ventral opening of the central pore with little or no stabilization by the B subunits. Although this tetrapeptide is clearly visible in the electron-density map of CT (Figure 8), the corresponding residues are disordered in the crystal structure of LT. This presumably reflects the more compact nature of CT's A2 chain (α-helix) which shelters the KDEL residues further within the protective confines of the pentamer pore. Deletion of these terminal four residues has little effect on B subunit oligomerization but significantly reduces the stability of the holotoxin (Streatfield *et al*., 1992). The

in vivo effect of such a deletion on toxin potency is not known.

Despite the relatively small size of the A2 chain, it shares an extensive interface with the A1 chain (Figure 4). The long amino-terminal A2 helix (residues 196 to 228) lies in a shallow groove that extends from one corner of the A1 subunit to the A1/B pentamer interface. Although after nicking the disulfide bridge between A1(Cys187) and A2(Cys199), which is the sole covalent anchor between the A1 and A2 chains, there are multiple non-polar interactions throughout the length of the interface. The carboxyl terminus of the A1 chain and the amino terminus of the A2 chain are partially disordered in the electron-density map, suggesting that this region contributes minimally to the stability of the nicked A subunit.

The A subunit/B pentamer interface

The arrangement of the B subunits in choleragen differs only modestly from that described for choleragenoid (Zhang *et al*., 1995). The presence of the A chain perturbs only those B side-chains that extend into the pentamer's central pore or that lie directly at the A/B interface. The A subunit does not appear to have any structural or functional bearing on the ganglioside-binding sites which lie on the remote outer edge of each B subunit (Figure 9).

Few direct stabilizing interactions occur between the A1 chain and the B pentamer. Exceptions include three arginine side-chains (Arg33, Arg143, and Arg148) located along the ventral surface of the A1 subunit that form multiple hydrogen bonds with carbonyl and glutamyl oxygen atoms located along the top of the pentamer's central α-helices (OThr78, OGlu79, $O^{\epsilon 1}$ and $O^{\epsilon 2}$Glu79). Since these contacts are all located adjacent to the axis of the pore, substantial rotation of the A subunit with regard to the B pentamer is possible without disruption of the interface (Sixma *et al*., 1992).

In contrast to the A1 chain, the A2 chain intimately interacts with all five B subunits (Figure 9). The A2 subunit passes through the central pore of the B pentamer either as a continuous helix (CT) or as an extended chain anchored at its carboxyl terminus by a short turn of helix (LT). The pore diameter is just sufficiently wide to accommodate the A2 chain as a helix, therefore, choleragen's A subunit displaces many of the solvent molecules noted to fill the choleragenoid pore (Zhang *et al*., 1995). Stabilizing contacts within the pore between the A2 chain and the B subunits are largely hydrophobic with very few specific hydrogen bonds noted at the resolution of the current structure. Surprisingly, the presence or absence of the A subunit has little effect on the stability of the B pentamer. This indicates a trade-off between intrapentameric and intersubunit bonds at the A/B interface (van Heyningen, 1982).

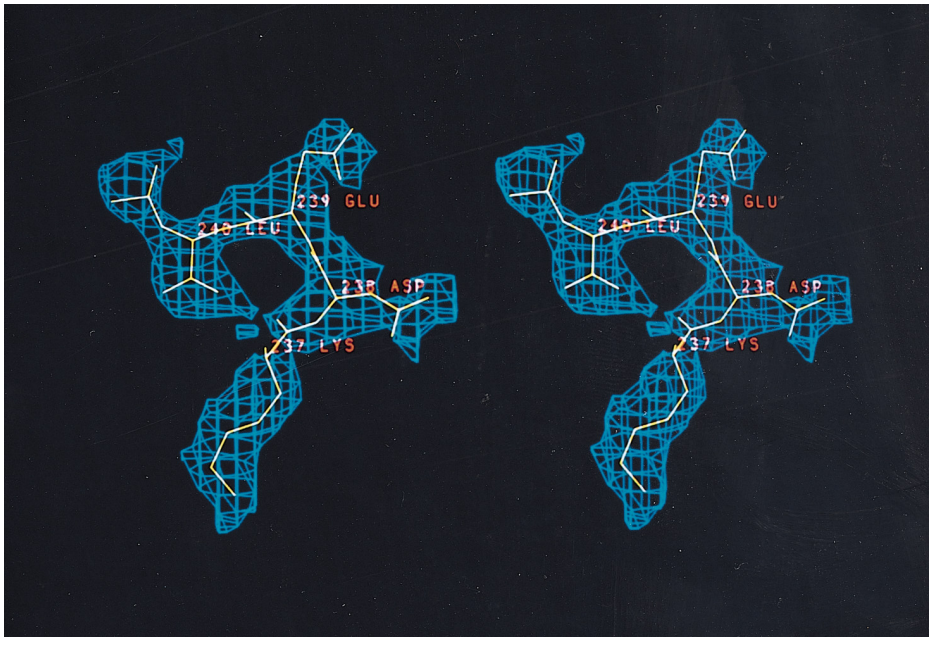

Figure 8. The carboxyl terminus of the A2 peptide—the KDEL sequence. The electron-densities for the terminal four residues of cholera toxin's A2 chain are relatively weak but easily interpretable. These four residues, which are disordered in the crystal structure of LT (Sixma *et al.*, 1993), lie just outside the ventral opening of the pentamer's central channel. The carboxyl KDEL sequence (or its analogue HDEL in LT) has been suggested to serve as a signal for retention of proteins in the endoplasmic reticulum (Joseph *et al.*, 1978, 1979). This tetrapeptide is important in maintaining the stability of the AB_5 holotoxin but is not essential for promoting B subunit oligomerization (Streatfield *et al.*, 1992). Whether the KDEL sequence plays a functional role in toxin internalization is unclear but this peptide is likely to be in contact with the membrane surface after CT is bound to GM_1 gangliosides.

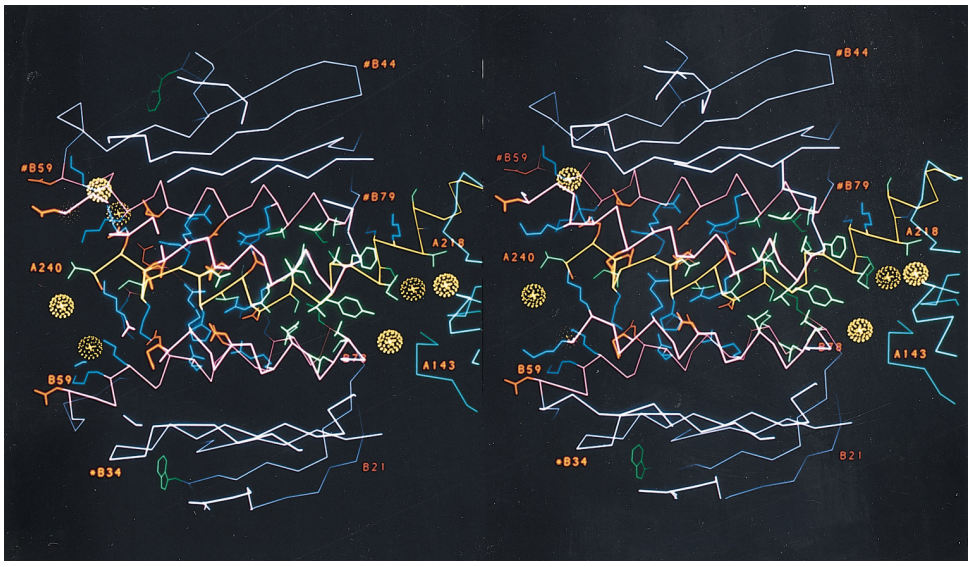

Figure 9. Cross-section through the central ''channel'' of choleragen. The A1 chain, A2 chain, and the B subunits are colored cyan, gold, and lavender, respectively. Side-chains contributing to the A2/B interface are shaded according to charge potential: green, non-polar; red, negatively charged; blue, positively charged. The Trp88 of opposed B subunits are shown to assist with orientation. Yellow spheres represent well-resolved water molecules. The A2/B interface is initially quite non-polar but becomes quite polar deeper in the channel. The carboxyl terminus of the A2 chain presumably interacts with the surface of the membrane during GM_1 binding. The sequence of the terminal four residues (KDEL) is identical to that shown to act as endoplasmic retention signal (Lewis & Pelham, 1990; Joseph *et al.*, 1978, 1979).

Mechanism of action

The route by which the A1 fragment crosses the membrane into the cytoplasm is not known. The structure of the choleragenoid-GM_1 pentasaccharide complex (Merritt *et al*., 1994a) and recent electron micrographs of choleratoxin (model membrane complexes: Cabral-Lilly *et al*., 1994) argue for the holotoxin binding to the membrane with the A subunit pointing away from the cell. This orientation is supported by immunological experiments indicating that the A1 fragment of the surface-bound or surface-assembled holotoxin is accessible to anti-A1 antibodies (Orlandi & Fishman, 1993; Jacob *et al*., 1984). Given the structural stability of the B pentamer, it is unlikely that the pentamer dissociates to provide a larger pore for passage of the A1 subunit. Internalization of the toxin must, therefore, be dependent upon some form of endocytosis that is perhaps mediated by the KDEL terminus of the A2 chain (Rothman & Orci, 1992; Lewis & Pelham, 1990). Cholera toxin coupled to horse-radish peroxidase (HRP) was visualized in the Golgi-endoplasmic reticulum-lysosomal system of cultured cells within one hour of incubation at 37°C. The entry of the toxin-HRP conjugate appeared not to occur through coated pits and was negligible at 4°C (Joseph *et al*., 1978; Tran *et al*., 1987).

Given the strong structural resemblance between CT and LT, it is worthwhile to note that the diseases associated with these toxins are quantitatively quite different. Whereas cholera is a fulminant disease that can be fatal within a few hours, the diarrhea caused by enterotoxic strains of *E. coli* is generally only a transitory cause of adult morbidity. The reasons for this disparity are not clear. Possibilities include modest structural changes in the toxins, differences in toxin secretion, or variation in microbial ecology. Further work will be needed to clarify the precise mechanism of these toxins and to pinpoint the weaknesses of these potent, highly evolved toxins.

Materials and Methods

Crystals of choleragen (0.3 mm × 0.3 mm × 0.3 mm) were grown from batches of freshly isolated, isoelectrically pure cholera toxin (Sigler *et al*., 1977; Spangler & Westbrook, 1989). The crystals are of space group $P2_1$, $a = 73.0$ Å $b = 92.2$ Å $c = 60.6$ Å $\alpha = 90.0°$ $\beta = 106.4°$ $\gamma = 90.0°$ with one AB_5 hexamer in the asymmetric unit. Native diffraction data were collected to a nominal resolution of 2.5 Å with a Siemens-Xentronics multiwire proportional counting detector using graphite monochromated radiation from a Rigaku RU-200 rotating anode generator operating at 5 kW. Molecular replacement with the computer program MERLOT (Fitzgerald, 1988) correctly positioned the refined coordinates of the choleragenoid B pentamer (Zhang *et al*., 1995) into the $P2_1$ cell. Conservative rigid body and least-squares refinements of the molecular replacement model reduced the crystallographic *R*-factor to below 30% (Finzel, 1987; Brunger *et al*., 1987). Three heavy-atom derivatives were prepared by conventional soaking techniques after the electron-density map calculated from the inverse Fourier transformation of the partial structure failed to provide an unambiguous interpretation of the A subunit (Table 1). Heavy-atom-binding sites and occupancies were refined with a modified version of PHARE (Otwinowski, 1993) that (1) used anisotropic temperature factors to better resolve closely spaced or clustered sites, and (2) reduced the bias contributed by a particular heavy-atom to its own refinement. Although MIR phasing alone gave a figure of merit of only 45% at 2.7 Å, the combination of MIR phases

Table 1. Crystallographic statistical summaries

A. *X-ray data collection summary*

Data set	Resolution cutoff (Å)	Number of data recorded	Number of unique data	Completeness (%)	R_{merge} (%)
Native	2.40	60,810	26,200	88.4	4.80
$NaAuI_4$	2.74	34,278	14,700	80.0	10.60
K_2PtCl_4	2.74	34,717	15,214	82.6	6.95
K_2OsO_4	3.44	17,988	8769	84.2	7.22

$R_{merge} = \Sigma|F_i - F|/\Sigma F_i$, where F_i are repeated measurements of equivalent structure factor amplitudes and F is the average value of F_i.

B. *Multiple isomorphous replacement of intact cholera toxin (choleragen)*

Parameter / Resolution	11.11	7.69	5.88	4.76	4.00	3.44	3.03	2.70	Overall
Figure of merit[a]	0.64	0.65	0.63	0.51	0.47	0.45	0.34	0.25	0.45
Phasing power[b]									
$NaAuI_4$	1.55	2.05	1.86	1.20	1.03	1.05	0.88	0.79	1.12
K_2PtCl_4	1.00	0.78	1.01	1.09	1.17	1.44	—	—	1.10
K_2OsO_4	1.20	1.34	1.49	1.07	0.96	1.00	1.20	1.04	1.09

[a] Figure of merit is a measure of the relative reliability of a phase based on the consistency of the MIR analysis from one derivative to the next. The maximum value is 1.0.

[b] $\Sigma|F_h^c|/\Sigma\|F_p^o|\exp(i\theta_c) + F_h^c| - |F_{ph}^o\|$, where $|F_h^c|$ is the calculated structure factor amplitude of the heavy atom, $|F_p^o|$ and $|F_{ph}^o|$ are the observed structure factor amplitudes of, respectively, the protein and the heavy-atom derivative, and θ_c is the calculated phase angle for the structure factor of the native protein crystal. The sum is taken over all reflections within the given resolution range.

C. *Refinement results*

Number of non-hydrogen atoms:	6136
Number of water atoms	138
Number of structure factors	26,200
Resolution limit (Å)	2.4
Crystallographic *R*-factor (%)	18.5
Deviations from ideal values (Å):	
Bond lengths:	0.015
Bond angle distances:	0.032
Planarity	0.045

with those from molecular replacement of the B pentamer provided a readily interpretable electron-density map. An iterative process of simulated annealing refinement of the initial AB_5 model with the computer package X-PLOR (Brunger *et al*., 1987), followed by density modification through solvent-flattening (Wang, 1985), improved the map quality sufficiently to visualize most side-chains. Interpretation of a few small areas of ambiguous density benefitted from comparison with the published structure of the heat-labile enterotoxin (Sixma *et al*., 1991). After multiple rounds of manual rebuilding and least-squares refinement with PROFFT (Finzel *et al*., 1987), the crystallographic *R*-factor for all data from 10 to 2.4 Å is 18.5%. On average, bond lengths, bond angle distances, and planarity deviated from ideal values by less than 0.015, 0.032, and 0.045 Å, respectively.

Acknowledgements

The coordinates will be deposited in the Brookhaven Protein Data Bank and are available directly from the authors on request until they have been processed and released. We thank Drs Prakas Maulik and Robert Reed of Boston University for collaborating on the structure of choleragenoid (B pentamer). Dr Paul. B. Sigler, of Yale University, generously provided computational and graphics facilities during a portion of this work. This work was supported by the National Institutes of Health through grants R01 AI28535 and R01 HL26335, and by the U.S. Department of Energy, Office of Health and Environmental Research through contract W-31-109-ENG-38.

References

Allured, V. S., Collier, R. J., Carroll, S. F. & McKay, D. B. (1986). Structure of exotoxin A of *Pseudomonas aeruginosa* at 3.0 Å resolution. *Proc. Natl Acad. Sci. USA*, **83**, 1320–1324.

Brunger, A. T., Kuriyan, J. & Karplus, M. (1987). Crystallographic *R*-factor refinement by molecular dynamics. *Science*, **235**, 458–460.

Burnette, W. N. (1994).AB_5 ADP-ribosylating toxins: comparative anatomy and physiology. *Structure*, **2**, 151–158.

Burnette, W. N., Mar, V. L., Plater, B. W., Schlotterbeck, J. D., McGinley, M. D., Stoney, K. S., Rohde, M. F. & Kaslow, H. R. (1991). Site-directed mutagenesis of the catalytic subunit of cholera toxin: substituting lysine for arginine 7 causes loss of activity. *Infect. Immunol.* **59**, 4266–4270.

Cabral-Lilly, D., Sosinsky, G. E., Reed, R. A., McDermott, M. R. & Shipley, G. G. (1994). Orientation of a cholera toxin bound to model membranes. *Biophys. J.* **66**, 935–941.

Carroll, S. F. & Collier, R. J. (1987). Active site of *Pseudomonas aeruginosa* exotoxin A. *J. Biol. Chem.* **262**, 8707–8711,

Cassel, D. & Pfeuffer, T. (1978). Mechanism of cholera toxin action: covalent modification of the guanyl nucleotide-binding protein of the adenylate cyclase system. *Proc. Natl Acad. Sci. USA*, **75**, 2669–2673.

Choe, S., Bennett, M. J., Fujii, G., Curmi, P. M. G., Kantardjieff, K. A., Collier, R. J. & Eisenberg, D. (1992). The crystal structure of diphtheria toxin. *Nature*, **357**, 216–222.

Dallas, W. S. (1983). Conformity between heat-labile toxin genes from human and porcine enterotoxigenic *Escherichia coli*. *Infect. Immun.* **40**, 647–652.

Dallas, W. S. & Falkow, S. (1980). Amino acid sequence homology between cholera toxin and *Escherichia coli* heat-labile toxin. *Nature*, **288**, 499–501.

De, S. N. (1959). Enterotoxicity of bacteria-free culture-filtrate of *Vibrio cholerae*. *Nature*, **183**, 1533–1534.

Dykes, C. W., Halliday, I. J., Hobden, A. N., Read, M. J. & Harford, S. (1985). A comparison of the nucleotide sequence of the A subunit of heat-labile enterotoxin and cholera toxin. *FEMS* family. In *Immunochemical and Molecular Genetic Analysis of Bacterial Pathogens* (Owen, P. & Foster, T. J. eds), vol. 85, Elsevier Science Publishers, New York.

Finkelstein, R. A. (1988). Cholera, the cholera enterotoxins, and the cholera enterotoxin-related enterotoxin. In *Immunochemical and Molecular Genetic Analysis of Bacterial Pathogens* (Owens, P. & Foster, T. J., eds), chapt. 7, pp. 85–102, Elsevier Science Publishers, New York.

Finzel, B. C. (1987). Incorporation of fast Fourier transforms to speed restrained least-squares refinement of protein structures. *J. Appl. Crystalog.* **20**, 53–55.

Fishman, P. H., Moss, J. & Osborne, J. C., Jr (1978). Interaction of choleragen with the oligosaccharide of ganglioside GM_1: evidence for multiple oligosaccharide binding sites. *Biochemistry*, **17**, 711–716.

Fitzgerald, P. M. D. (1988). MERLOT, an integrated package of computer programs for the determination of crystal structures by molecular replacement. *J. Appl. Crystallog.* **21**, 273–278.

Foster, J. W. & Kinney, D. M. (1985). ADP-ribosylating microbial toxins. *CRC Crit. Rev. Microbiol.* **11**, 273–298.

Fraser, M. E., Chernaia, M. M., Kozlov, Y. V. & James, M. N. G. (1994). Crystal structure of the holotoxin from *Shigella dysenteriae* at 2.5 Å resolution. *Struct. Biol.* **1**, 59–64.

Galloway, T. S. & van Heyningen, S. (1987). Binding of NAD^+ by cholera toxin. *Biochem. J.* **244**, 225–230.

Gill, D. M. (1975). Involvement of nicrotinamide adenine nucleotide in the action of cholera toxin *in vitro*. *Proc. Natl Acad. Sci. USA*, **72**, 2064–2068.

Gill, D. M. & Coburn, J. (1987). ADP-ribosylation by cholera toxin: functional analysis of a cellular system that stimulates the enzymatic activity of cholera toxin fragment A_1. *Biochemistry*, **26**, 6364–6371.

Harford, S. C., Dykes, W., Hobden, A. N., Read, H. J. & Halliday, I. J. (1989). Inactivation of the *Escherichia coli* heat-labile enterotoxin by *in-vitro* mutagenesis of the A-subunit gene. *Eur. J. Biochem.* **183**, 311–316.

Jacob, C. O., Sela, M., Pines, M., Hurwitz, S. & Arnon, R. (1984). Neutralization of heat-labile toxin of *E. coli* by antibodies to synthetic peptides derived from the B subunit of cholera toxin. *Proc. Natl Acad. Sci. USA*, **81**, 7893–7896.

Janicot, M., Fouque, F. & Desbuqois, B. (1991). Activation of rat liver adenylate cyclase by cholera toxin requires toxin internalization and processing in endosomes. *J. Biol. Chem.* **266**, 12858–12865.

Joseph, K. C., Kim, S. U., Steiber, A. & Gonatas, N. K. (1978). Endocytosis of cholera toxin into neuronal GERL. *Proc. Natl Acad. Sci. USA*, **75**, 2815–2819.

Jospeh, K. C., Steiber, A. & Gonatas, N. K. (1979). Endocytosis of cholera toxin in GERL-like structures of murine neuroblastoma cells pretreated with GM_1 ganglioside. *J.Cell Biol.* **81**, 543–554.

Kassis, S., Hagmann, J., Fishman, P. H., Chang, P. P. & Moss, J. (1982). Mechanism of action of cholera toxin on intact cells. Generation of A1 peptide and activation of adenylate cyclase. *J. Biol. Chem.* **257**, 12148–12152.

Kurosky, A., Markel, D. E. & Peterson, J. W. (1977). Covalent structure of the B chain of cholera enterotoxin. *J. Biol. Chem.* **252**, 7257–7264.

Lai, C.-Y., Xia, Q.-C. & Salotra, P. T. (1983). Location and amino acid sequence around the ADP-ribosylation site in the cholera toxin active subunit A1. *Biochem. Biophys. Res. Commun.* **116**, 341–348.

Lewis, M. J. & Pelham, H. R. B. (1990). A human homologue of the yeast HDEL receptor. *Nature*, **348** 162–163.

Lockman, H. & Kaper, J. B. (1983). Nucleotide sequence analysis of the A2 and the B subunits of *Vibrio cholerae* enterotoxin. *J. Biol. Chem.* **258**, 13722–13726.

Ludwig, D. S., Ribi, H. O., Schoolnik, G. K. & Kornberg, R. D. (1986). Two-dimensional crystals of cholera toxin B-subunit-receptor complexes: projected structure at 17-Å resolution. *Proc. Natl Acad. Sci. USA*, **83**, 8585–8588.

McDaniel, R. V. & McIntosh, T. J. (1986). X-ray diffraction studies of the cholera toxin receptor, GM_1. *Biophys. J.* **49**, 94–96.

Mekalanos, J. J., Collier, R. J. & Romig, W. R. (1979). Enzymatic activity of cholera toxin. II. Relationships of proteolytic processing, disulfide bond reduction, and subunit composition. *J. Biol. Chem.* **254**, 5855–5861.

Mekalanos, J. J., Swartz, D. J., Pearson, G. D. N., Harford, N., Groyne, F. & De Wilde, M. (1983). Cholera toxin genes: nucleotide sequence, deletion analysis and vaccine development. *Nature*, **306**, 551–557.

Merritt, E. A., Sarfaty, S., van den Akker, F., L'hoir, C. L., Martial, J. A. & Hol, W. G. J. (1994a). Crystal structure of cholera toxin B-pentamer bound to receptor GM1 pentasaccharide. *Protein Sci.* **3**, 166–175.

Merritt, E. A., Pronk, S. E., Sixma, T. K., Kalk, K. H., van Zanten, B. A. & Hol, W. G., (1994b). Structure of partially-activated *E. coli* heat-labile enterotoxin (LT) at 2.6 Å resolution. *FEBS Letters* **337**, 88–92.

Moss, J. & Vaughan, M. (1988). ADP-ribosylation of guanyl nucleotide-binding regulatory proteins by bacterial toxins. *Advan. Enzymol.* **61**, 303–379.

Moss, J. & Vaughan, M. (1991). Activation of cholera toxin and *Escherichia coli* heat-labile enterotoxins by ADP-ribosylation factors, a family of 20 kDA guanine nucleotide-binding proteins. *Mol. Microbiol.* **5**, 2621–2627.

Moss, J., Manganiello, V. C. & Vaughan, M. (1976). Hydrolysis of nicotinamide adenine nucleotide by choleragen and its A promoter: possible role in activation of adenylate cyclase. *Proc. Nat Acad. Sci. USA*, **73**, 4424–4427.

Moss, J., Tsai, S. C. & Vaughan, M. (1994). Activation of cholera toxin by ADP-ribosylation factors. *Methods Enzymol.* **235**, 640–647.

Mosser, G., Mallouh, V. & Brisson, A. (1992). A 9 Å two-dimensional projected structure of cholera toxin B-subunit-GM_1 complexes determined by electron crystallography. *J. Mol. Biol.* **226**, 23–28.

Orlandi, P. A. & Fishman, P. H. (1993). Orientation of

cholera toxin bound to target cells. *J. Biol. Chem.* **268**, 17038–17044.

Otwinowski, Z. (1991). In *Isomorphous Replacement and Anomalous Scattering: Proceedings of the CCP4 Study Weekend 25–26 January 1991* (Wolf, W., Evans, P. R. & Leslie, A. G. W., eds), pp. 80–86, SERC, Darebury Laboratory, Warrington.

Peterson, W. J. & Ochoa, L. G. (1989). Role of prostaglandins and cAMP in the secretory effects of cholera toxin. *Science*, **245**, 857–859.

Reed, R. A., Mattai, A. J. & Shipley, G. G. (1987). Interaction of cholera toxin with ganglioside GM1 receptors in supported lipid monolayers. *Biochemistry*, **26**, 824–832.

Ribi, H. O., Ludwig, D. S., Mercer, K. L., Schoolnik, G. K. & Kornberg, R. D. (1988). Three-dimensional structure of cholera toxin penetrating a lipid membrane. *Science*, **239**, 1272–1276.

Richards, F. M. & Kundrot, C. E. (1988). DEFINE_Structure: a program for specification of secondary and first level supersecondary structure from alpha carbon coordinate list. *Proteins: Struct. Funct. Genet.* **3**, 71–84.

Rothman, J. E. & Orci, L. (1992). Molecular dissection of the secretary pathway. *Nature*, **355**, 409–415.

Sattler, J., Schwarzmann, G., Knack, I., Rohm, K.-H. & Wiegandt, H. (1978). Studies of ligand binding to cholera toxin III, cooperativity of oligosaccharide binding. *Hoppe-Seyler's Z. Physiol. Chem.* **359**, 719–723.

Sigler, P. B., Druyan, M. E., Kiefer, H. C. & Finkelstein, R. (1977). Cholera toxin crystals suitable for X-ray diffraction studies. *Science*, **197**, 1277–1279.

Sixma, T. K., Pronk, S. E., Kalk, K. H., Wartna, E. S., Van Zanten, B. A. M., Witholt, B. & Hol, W. G. J. (1991). Crystal structure of a cholera toxin-related heat-labile enterotoxin from *E. coli*. *Nature*, **351**, 371–378.

Sixma, T. K., Aguirre, A., Terwisscha van Scheltinga, A. C., Wartna, E. S., Kalk, K. H. & Hol, W. G. J. (1992a). Heat-labile enterotoxin crystal forms with variable A/B_5 orientation. *FEBS Letters*, **305** , 81–85.

Sixma, T. K., Pronk, S. E., Kalk, K. H., van Zenten, B. A. M., Berhuis, A. M. & Hol, W. J. G. (1992b). Lactose binding to heat-labile enterotoxin revealed by X-ray crystallography. *Nature*, **355**, 561–564.

Sixma, T. K., Kalk, K. H., van Zanten, B. A. M., Dauter, Z., Kingma, J., Witholt, B. & Hol, W. G. J. (1993). Refined crystal structure of *Escherichia coli* heat-labile enterotoxin, a close relative of cholera toxin. *J. Mol. Biol.* **230**, 890–918.

Spangler, B. D. (1992). Structure of function of cholera toxin and the related *Escherichia coli* heat-labile enterotoxin. *Microbiol. Rev.* **56**, 622–647.

Spangler, B. D. & Westbrook, E. M. (1989). Crystallization of isoelectrically homogenous cholera toxin. *Biochemistry*, **28**, 1333–1340.

Stein, P. E., Boodhoo, A., Tyrell, G. J., Brunton, J. L. & Read, R. J. (1992). Crystal structure of the cell-binding B oligomer of verotoxin-1 from *E. coli*. *Nature*, **355**, 748–750.

Stein, P. E., Boodhoo, A., Armstrong, G. D., Cockle, S. A., Kelin, M. H. & Read, R. J. (1994). The crystal structure of pertussis toxin. *Structure*, **2**, 45–57.

Streatfield, S. J., Sandkvist, M., Sixma, T. K., Bagdasarian, M., Hol, W. G. & Hirst, T. R. (1992). Intermolecular interactions between the A-subunit and B-subunit of heat-labile enterotoxins from *Escherichia coli* promote holotoxin assembly and stability *in-vitro*. *Proc. Natl Acad. Sci, USA*, **89**, 12140–12144.

Surewicz, W. K., Leddy, J. J. & Mantsch, H. H. (1990). Structure, stability and receptor interaction of cholera toxin as studied by Fourier-transform infrared spectroscopy. *Biochemistry*, **29**, 8106–8111.

Tomasi, M., Battistini, A., Araco, A., Roda, L. G. & D'Agnolo, M. (1979). The role of the reactive disulfide bond in the interaction of cholera toxin functional regions. *Eur. J. Biochem.* **93**, 621–627.

Tran, D., Carpentier, J.-L., Sawano, F., Gorden, P. & Orci, L. (1987). Ligands internalized through coated or non-coated invaginations follow a common intracellular pathway. *Proc. Natl Acad. Sci. USA*, **84**, 7957–7961.

Tsuji, T., Honda, T., Miwatani, T., Wakabayashi, T. & Matsubara, H. (1984). The amino acid sequence of the B-subunit of porcine *Escherichia coli* enterotoxin. *FEMS Microbiol. Letters*, **25**, 243–246.

Tsuji, T., Inoue, T., Miyama, A. & Noda, M. (1991). Glutamic acid-112 of the A subunit of heat-labile enterotoxin from enterotoxigenic *Escherichia coli* is important for ADP-ribosyltransferase. *FEBS Letters*, **291**, 319–321.

van Heyningen, S. (1982). Conformational changes in subunit A of cholera toxin following the binding of ganglioside to subunit B. *Eur. J. Biochem.* **122**, 333–337.

Wang, B.-C. (1985). Resolution of phase ambiguity in macromolecular crystallography. *Methods Enzymol.* **115**, 90–117.

Yang, J., Tamm, L. K., Tillack, T. W. & Shao, Z. (1993). New approach for atomic force microscopy of membrane proteins. The imaging of cholera toxin. *J. Mol. Biol.* **229**, 286–290.

Zhang, R.-G., Westbrook, M. L., Westbrook, E. M., Scott, D. L., Otwinowski, Z., Maulik, P. R., Reed, R. A. & Shipley, G. G. (1995). The 2.4 Å crystal structure of cholera toxin B subunit pentamer: choleragenoid. *J. Mol. Biol*. In the press.

Edited by R. Huber

(Received 12 December 1994; accepted in revised form 5 June 1995)